
The Influx of Comets and Asteroids to the Earth

D. W. Hughes

Phil. Trans. R. Soc. Lond. A 1981 **303**, 353-368

doi: 10.1098/rsta.1981.0209

Email alerting service

Receive free email alerts when new articles cite this article - sign up in the box at the top right-hand corner of the article or click [here](#)

To subscribe to *Phil. Trans. R. Soc. Lond. A* go to: <http://rsta.royalsocietypublishing.org/subscriptions>

The influx of comets and asteroids to the Earth

BY D. W. HUGHES

Department of Physics, University of Sheffield, Sheffield S3 7RH, U.K.

Knowledge of the size distribution of comets and asteroids can be obtained from two sources. First the planet Earth can be regarded as a detector and the diameter distribution of Earth craters used to assess the mass distribution of the incident bodies. Secondly observations from Earth of the characteristics and orbits of comets and asteroids can lead to their collision probabilities and mass distributions. Simplistically it can be stated that the Earth craters have been produced by small incident objects whereas the comets and asteroids that are easily seen are the large ones. This paper seeks to relate these diverse sources of information.

INTRODUCTION

It is obvious that the Earth and the Moon (which is to all intents and purposes at the same heliocentric distance) are still being bombarded by comets and asteroids. The cumulative number – size curves for both comets and asteroids indicate that the incident numbers decrease drastically as the size increases. The objects that commonly hit Earth are the small ones. The comets and asteroids that are easily visible in the sky are the large ones. Our knowledge of the distribution of minor bodies is enhanced by interpolating between these extremes.

Three obvious events of Earth–Moon bombardment have occurred in recent history. There seems to be a reasonable possibility that the lunar crater Giordano Bruno (latitude 30°N , longitude 103°E) was formed at about 20 45 min G.M.T. on 18 July 1178. Evidence for this has been presented by Hartung (1976), who retells the report of five men who happened to be looking at the 1.5 day old Moon when ‘suddenly the upper horn split in two. From the midpoint of this division a flaming torch sprang up, spewing out over a considerable distance fire, hot coals and sparks. Meanwhile the body of the Moon which was below writhed as it were in anxiety...and throbbed like a wounded snake’. Giordano Bruno has a very sharp crater rim which has not been rounded off by the ‘gardening’ process. It also has the largest ray length to crater diameter of all the lunar craters. The diameter is 20 km. The meteorite energy required to produce a terrestrial or lunar crater of diameter D m is about $4 \times 10^{13} D^3$ erg† (see Allen 1973). (Wood (1979) gives $1.6 \times 10^{13} D^{3.6}$ erg and Dence *et al.* (1977) find $6.4 \times 10^{12} D^{3.4}$ erg.) If a projectile density of 3 g cm^{-3} is assumed, the Allen relation gives the ratio of projectile diameter to crater diameter as 30, 62 and 99 for incident velocities of 12, 35 and 70 km s^{-1} respectively. The object responsible for Giordano Bruno was thus probably less than 1 km across.

The Barringer crater near Flagstaff, Arizona, is a typical, new, Earth crater. This has a diameter of 1.22 km and the crater floor is 0.184 km below the rim. The desert around the crater is strewn with about 30 t of iron meteorite fragments. The most likely age is about 50 000 a‡ (see Vdovykin 1973). From the Allen relation, the mass of the causative object of diameter d cm is $8 \times 10^7 d^3 v^2$, where v is the impact velocity (cm s^{-1}). This gives a mass of 10^{11} g for a v of 12 km s^{-1} . The ‘out of atmosphere’ values of mass and velocity would be higher than this as the ablation and retardation in the atmosphere is significant.

† 1 erg = 10^{-7} J.

‡ The symbol a stands for year; 1 Ma = 10^6 a; 1 Ga = 10^9 a.

For the Tunguska object this ablation and retardation was so dominant that all the energy was dissipated in the atmosphere and only a few cosmic spherules hit the ground. The Tunguska explosion took place at about 07 h 17 min local time on 30 June 1908. An explosion of about 5×10^{23} erg led to a devastation of the Siberian taiga over an area of diameter 70 km. The centre of the damaged area had been ravaged by fire, searing being traceable for 18 km. Even though the surface damage was extensive no specific crater was found. The main explosion occurred at a height of 8.5 km above the ground.

Brown & Hughes (1977) concluded that an impacting comet was responsible. By assuming that the original kinetic energy was entirely converted into explosive energy, the cometary nucleus is found to have a mass of 5×10^{10} g and a diameter of about 40 m. The absolute magnitude of the comet (the magnitude that it would have if it were 1 AU away from both the Sun and the Earth) was calculated to be +26. The fact that it was extremely faint, had already passed perihelion and hit the Earth from the solar direction amply explains why no one actually detected the comet in space.

Meteorite falls are fairly common. The word 'fall' denotes the meteorite fragments that survive the passage through the atmosphere and, after landing, are large enough to be found and picked up. About 3300 meteorites hit the Earth's surface each year but unfortunately only about 6 are picked up.

This paper reviews the influx rates of the minor objects in the Solar System to the Earth's surface and contrasts the populations of the Earth impacts with the populations in for example the comet cloud and the asteroid belt.

THE INFLUX RATE

A reasonable estimate can be made of the influx of asteroid-like, crater-producing bodies to the Earth's surface. Figure 1 shows the worldwide distribution of impact craters, these data coming from Grieve & Robertson (1979).



FIGURE 1. The worldwide distribution of impact craters (after Grieve & Robertson 1979).

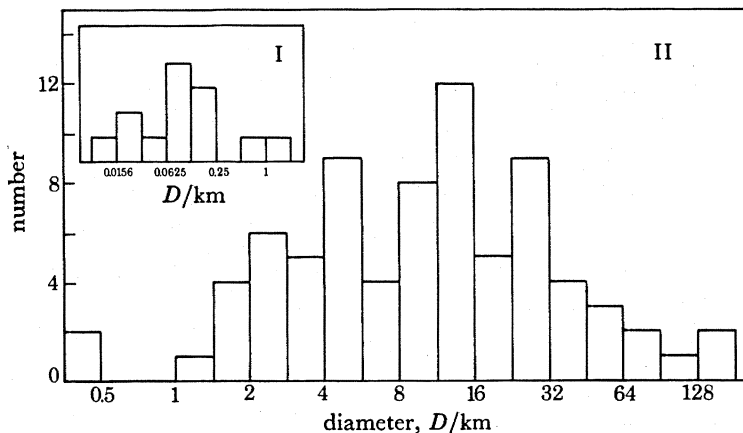


FIGURE 2. The diameter distribution of impact craters. Group I are proven meteorite craters; group II are probable impact craters.

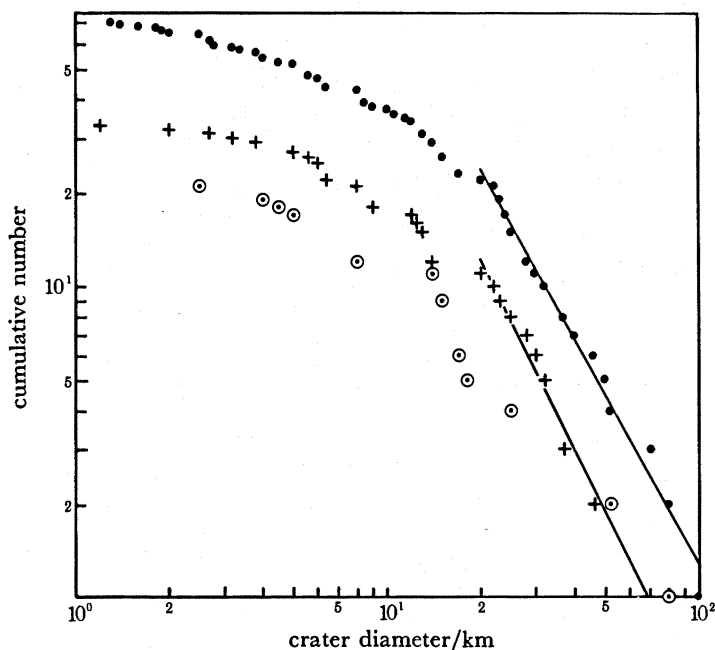


FIGURE 3. The cumulative numbers of Phanerozoic craters as a function of diameter: ● the world total; + craters on the North American stable region; ⊙ craters on the Eo-European craton (these data come from Grieve & Robertson 1979).

Twelve of the structures shown in figure 1 are classified as proven meteorite craters because meteorite fragments have been found in their vicinity. The remaining 75 are 'probable' meteorite craters recognized as such because the target rocks have suffered shock metamorphic effects. It is obvious from the uneven distribution that the probability of their preservation and detection varies considerably from place to place. The majority occur in North America and Europe, areas with relatively stable geology and also with an active population of crater searchers. Erosion and geological processes progressively erase craters. For example a 20 km structure is only recognizable as a probable impact crater for a maximum of 600 Ma whereas a 10 km structure usually has a lifetime of only 300 Ma.

Figure 2 shows the distribution of crater diameters. A cumulative plot of the world population of Phanerozoic craters with diameters greater than 10 km is given in figure 3, the data coming from Grieve & Dence (1979). The cumulative number, N , is proportional to $D^{-1.81}$ for $D > 20$ km. Large lunar craters lie between $N \propto D^{-1.8}$ (Baldwin 1971) and $N \propto D^{-2}$ (Hartmann & Wood 1971) and Martian craters also obey an $N \propto D^{-2}$ law (Neukum & Wise 1976). The change in slope at a crater diameter of about 20 km is due to the variation of crater lifetime as a function of diameter. It is to be expected that the slope of the $D > 20$ km line represents the true size distribution and one that can be extrapolated to diameters down to about 1 km.

To calculate the cratering rate one needs ideally a large area of the Earth's land mass that has a single age of origin, preferably as old as possible, and which has undergone a minimal and uniform level of subsequent modifying geological activity. Two areas approximate to this. The first is the North American stable region that lies between the Rockies and the Appalachians and the Quachita and the Arctic. The area is 1.25×10^7 km² and the exposure age varies from 450 Ma in the north to about 300 Ma in the south. It contains 33 impact structures over 1 km in diameter, the cumulative distribution of these being shown in figure 3. A linear regression analysis of the data for $D > 20$ km leads to the equation

$$\lg N = 3.74 - 2.04 \lg D. \quad (1)$$

We assume that all the craters larger than 20 km have been detected. From equation (1) it can be concluded that 12.2 craters with $D > 20$ km have been formed in an area of 1.25×10^7 km² over a period of about 375 Ma. The production rate of craters larger than 20 km turns out to be 2.6×10^{-15} km⁻² a⁻¹. The European crater distribution is also given in figure 3. As this data set is so meagre it has been added to the American one. The cumulative number equation is then

$$\lg N = 3.63 - 1.85 \lg D. \quad (2)$$

The resulting fit indicates that 16.75 craters larger than 20 km in diameter were formed in a total area of 1.7×10^7 km² again over 375 Ma. The rate is the same as that found above, and can be quoted as $(2.6 \pm 0.9) \times 10^{-15}$ km⁻² a⁻¹. The world cumulative curve given in figure 3 indicates that N is proportional to $D^{-1.81}$ for $D > 20$ km. Combining this with the production rate given above results in the equation

$$\lg \phi = -(12.23 \pm 0.16) - (1.81 \pm 0.07) \lg D, \quad (3)$$

where ϕ is the production rate (km⁻² a⁻¹) of craters with diameters greater than D km. This equation is definitely valid down to diameters of 20 km and probably valid down to diameters of 1 km. If the Earth's surface was all land, equation (3) leads to the prediction that a 1 km crater would be produced every 3000 a, a 10 km crater every 200 000 a and a 20 km crater every 800 000 a. We must be thankful that two-thirds of the globe is covered by water and, of the remaining land mass, the frozen wastes, jungles, deserts and mountains account for over 90% of the area.

Equation (3) can be extended in two ways. First it is important to realize that the cratering rate varies as a function of geological time. This is shown schematically in figure 4 (after Hartmann 1977). Intense bombardment obviously took place in the early days of the Solar System, during which time the planets were sweeping up the debris left over from the formation. New material is often injected into the system after the breakup of specific large asteroids. This is shown by the spikes in the downward curve.

The second extension introduces mass. Rewriting Wood's (1979) expression gives

$$E = 1.01 \times 10^{24} D^{3.6} \text{ erg}, \quad (4)$$

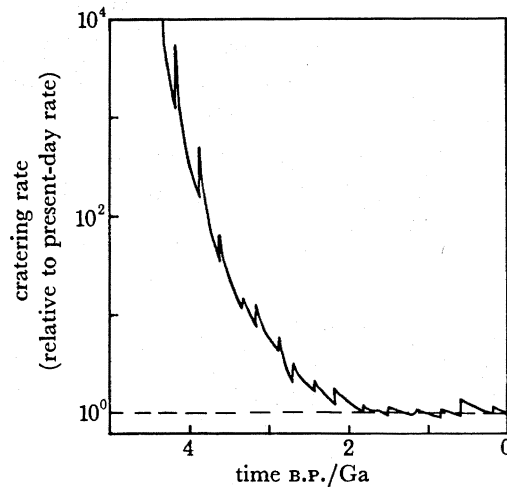


FIGURE 4. A schematic diagram showing how the rate of cratering has declined during the last 4.5×10^9 a (after Hartmann 1977).

where D is the crater diameter (km). If we assume that the energy of the causative projectile, E , is simply kinetic and that these crater producing objects have a mean velocity of 20 km s^{-1} on impact then substitution into equation (4) gives

$$m = 5.05 \times 10^{11} D^{3.6} \text{ g.} \quad (5a)$$

Substitution of equation (5a) into equation (3) gives

$$\lg \phi_E = 2.36 - 0.50 \lg m, \quad (6a)$$

where ϕ_E is the flux, per year, to the Earth's surface of objects that have masses greater than m g. Equation (6a) is valid over the mass range $2 \times 10^{16} < m < 10^{19}$ g, this being equivalent to crater diameters in the range $20 < D < 100$ km.

The relation between projectile energy and the resultant crater diameter is somewhat uncertain. Allen (1973) gives $E = 4 \times 10^{22} D^3$ erg (D in kilometres) and equations (5) and (6) thus become

$$m = 2 \times 10^{10} D^3 \text{ g} \quad (5b)$$

and

$$\lg \phi_E = 2.70 - 0.60 \lg m. \quad (6b)$$

Dence *et al.* (1977) give $D = 1.01 \times 10^{23} D^{3.4}$ erg (D in kilometres) resulting in

$$m = 5.07 \times 10^{10} D^{3.4} \text{ g,} \quad (5c)$$

$$\lg \phi_E = 2.18 - 0.532 \lg m. \quad (6c)$$

The mass distribution index, s , of a population of incident objects can be defined by the relation $\phi_E \propto m^{1-s}$. (An equivalent definition gives the number of objects with masses lying between the limits m and $m + dm$ as being proportional to m^{-s} .)

Equations (6) above lead to s values of 1.50, 1.60 and 1.53 respectively. Not only is scatter produced by the variations in the relations between E and D but also there is a scatter introduced by the standard deviations given in equation (3). This is equivalent to ± 0.02 in s value. Crudely we can write the mean s value of the incident object as 1.54 ± 0.05 . This will be compared with the mass distributions of asteroids and comets in a later section. The three flux curves (6) are plotted as a function of mass in figure 5.

The calculation of the influx to the Earth can be approached from an entirely different direction. Everhart (1969) has calculated how many planet-comet encounters occur when 10^9 hypothetical random parabolic comets interact with the Solar System. A fraction of these comets are captured by the large planets (Jupiter and Saturn mainly) into orbits with periods less than 200 a. Everhart also calculates how many of the 10^9 parabolic comets will hit the Earth per year. The Everhart flux can be represented by the equation

$$\lg \phi_E = -10.618 + 0.282 H_{10} \quad (13.9 > H_{10} > 7.9), \quad (7)$$

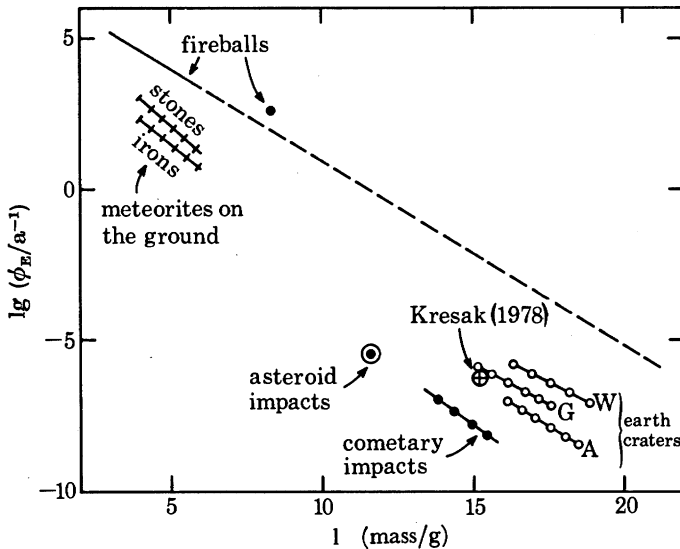


FIGURE 5. A logarithmic plot of the cumulative number of events occurring over the whole surface of the Earth per year as a function of mass. Meteorite data come from Hughes (1980a) and relate to the residue of objects that have survived passage through the atmosphere. The fireball data (Ceplecha 1976; McCrosky 1968) refer to the interplanetary mass of the meteorite parent body. The asteroid impact point results from an analysis of Earth-crossing asteroid orbits (see Shoemaker *et al.* 1979). The cometary impact line has been produced by Everhart (1969) and relies on the presupposition that there are 10^9 comets in the Oort/Öpik cloud. This line can thus be moved up the diagram by adjusting this assumption. The Earth-cratering lines have been obtained in this paper. The labels W, G and A relate to the Wood, Grieves & Dence and Allen relations between crater diameter and the energy of the causative body. The dashed line is an extrapolation of the fireball data.

where H_{10} is the absolute magnitude of the comet. The relation between the mass of a cometary nucleus and its H_{10} value has been given by R. Newburn Jr (private communication, 1979) as

$$\lg m = 19 - 0.4 H_{10}. \quad (8)$$

Substitution of this relation into equation (7) gives

$$\lg \phi_E = 2.78 - 0.71 \lg m \quad (15.8 > \lg m > 13.4). \quad (9)$$

This curve is also plotted in figure 5. Notice that the value of the first constant (2.78) depends directly on the assumed value for the number of interacting comets (10^9). Collisions will also take place between the Earth and the non-parabolic comets. Over the magnitude range $1 < H_{10} < 7$ it can be crudely estimated that there are about 30 parabolic comets visible from Earth for every one non-parabolic comet (see Hughes & Daniels 1980). However, the non-parabolic, inner Solar System comets have an average period of about 8 a, and so the chance of encounter

is thus greatly increased. A reasonable supposition, taking these two factors into account, is that the comet flux rate is between 10 and 100 times larger than the value given by equation (9).

The influx of asteroids has been estimated by Shoemaker *et al.* (1979). They consider Earth-crossing asteroids, defined as being all the asteroids that at any time during their life can be perturbed into orbits that intersect the orbit of the Earth. There are three basic groups. The Aten asteroids have orbits with semi-major axes (a) less than 1 AU and aphelion distances (q) greater than 0.983 AU (the Earth's perihelion distance). Three have been discovered since 1976. Apollo asteroids ($a \geq 1.0$ AU, $q \leq 1.017$ AU) overlap the Earth's orbit in the region of perihelion. Out of 22 known Apollos with reasonably well determined orbits 21 are Earth-crossing. Amor asteroids have perihelion distances q in the range 1.017 AU $< q < 1.3$ AU. They do not cross the Earth's orbit at the present time but secular perturbations can easily change their orbits into ones that do. Twenty are known. All known Earth-crossing asteroids have a finite probability of colliding with Earth. Shoemaker *et al.* (1979) find that the statistical distribution of orbital characteristics of the entire population of Earth-crossers is probably nearly in a steady state. They do not expect the collision rate to change appreciably with time, and stress that the present-day collision rate is probably representative of the rate for the past 10^7 a. Monte Carlo studies of collision and ejection probabilities indicate that the Earth-crossers have typical lifetimes of a few tens of millions of years (Wetherill 1976). The collision rates obtained by Shoemaker *et al.* (1979) are summarized in table 1. The final column is simply the product of the mean collision probability of each asteroid and the estimated population; $V(1, 0)$ is the absolute visual magnitude of the asteroid, defined as being its apparent magnitude when it is 1 AU from Earth and at zero phase angle. Table 1 indicates that 3.5 asteroids brighter than absolute magnitude 18 will hit the Earth every million years. One will be an Aten, two will be Apollos and one-half will be an Amor.

TABLE 1. COLLISION RATES WITH THE EARTH OF KNOWN CLASSES OF EARTH-CROSSING ASTEROIDS

(After Shoemaker *et al.* 1979.)

	estimated population down to $V(1, 0) = 18$	mean collision probability 10^{-9} a^{-1}	collision rate down to $V(1, 0) = 18$ 10^{-6} a^{-1}
Atens	<i>ca.</i> 100	9.1	0.9
Apollos	700 ± 300	2.6	1.8 ± 0.8
Earth-crossing Amors	<i>ca.</i> 500	<i>ca.</i> 1	<i>ca.</i> 0.5
total	<i>ca.</i> 1300		<i>ca.</i> 3.5

The conversion between absolute visual magnitude $V(1, 0)$ and mass can be approached in the following way. Zellner & Bowell (1977) give the asteroid diameter, D km, as

$$2 \lg \left(\frac{1}{2} D \right) = 5.642 - 0.4 V(1, 0) - \lg p_v, \quad (10)$$

where p_v is the geometric albedo. Morrison (1977*a*) finds that the number of carbonaceous asteroids exceeds the number of silicaceous asteroids by a factor of 7 ± 2 . Carbonaceous asteroids have a geometric albedo of about 0.035. Assuming that all incident asteroids are carbonaceous and of density 3 g cm^{-3} results in the restriction that $V(1, 0)$ is brighter than 18 being equivalent to diameters being greater than 0.062 km and masses in excess of $3.8 \times 10^{11} \text{ g}$. The Shoemaker *et al.* flux point is shown in figure 5. This point lies almost exactly and probably fortuitously on

the extrapolation of the Everhart comet data. Both comet and asteroid data lie considerably (approximately $1\frac{1}{2}$ orders of magnitude) below the influx rate estimated from crater counts. In dealing with the first point it must be stressed that we have relatively scant knowledge of ratios between the numbers of comets and asteroids of a specific mass hitting the Earth. Shoemaker estimates that the collision rate of active cometary nuclei is not more than about 10% of the collision rate of asteroids.

A third approach to this problem has been made by Kresak (1978*a, b*). He considered a specific region of space, this being centred on planet Earth and having a radius of 0.20 AU, and then listed the comets and asteroids that have entered this region during recent history. During the period 1677.0 to 1977.0 there have been 27 entries of 27 different long period comets ($p > 200$ a) and 14 entries of 11 short period comets ($p < 100$ a). In the 50 a between 1927.0 and 1977.0 there have been 19 entries of 10 Amor asteroids and 22 entries of 16 Apollo asteroids. The completeness of the sample was investigated by considering how the number of approaches varied as a function of the minimum miss distance (Δ_A). There should be a Δ_A^2 dependence. The time that the object spent in the region should vary as Δ_A^3 and the magnitude distribution indices should agree with those found for other comets and asteroids. The effects of observational selection were only too obvious.

It was found that the mass ranges of these comets and asteroids nearly coincided. Most of the long-period close-encounter comets were estimated to have diameters between 2 and 10 km. Most of the short-period comets and asteroids were in the $1 < D < 3$ km region. Kresak then concentrated on producing a bias-free estimation of the flux of these objects to the Earth. The effects of the gravitational attractions of the Earth were taken into account. The final conclusion was that the number of objects with diameters greater than 1 km that approach to within 0.1 AU of the Earth within a time period of 100 a was as follows: 2.5 long-period comets ($p > 200$ a), 1.2 short-period comets ($p < 200$ a), 20 to 30 asteroids of the Amor type and 120 to 170 asteroids of the Apollo type. Kresak found that the Earth would collide with a body (asteroid or cometary nucleus) with a diameter greater than 1 km every 1.5–2 Ma years. This data point is shown on figure 5 and is comfortably close to the Earth crater lines given earlier in this paper. Notice that Kresak gives the ratio of impacting asteroid to impacting comets ($D > 1$ km) as 46:1.

Wetherill (1979) finds that the cometary contribution is much more important. He investigated the steady-state population of Apollo–Amor objects and concluded that the number of Apollo asteroids should be about twice the number of Amor asteroids. The lifetime of minor bodies in the Solar System in planet-crossing orbits is, in the main, much less than the age of the Solar System (Öpik 1951). As these bodies obviously exist, there must be a source, a long-lived source, that replaces those lost by planetary impact and by ejection into heliocentric escape orbits. According to Wetherill the injection rate from this source needs to be about 15 objects per million years to maintain the present-day Apollo–Amor population. Comet Encke is the only known active comet in an Apollo-like orbit. If Encke's nucleus is about 1 km in diameter and this value is typical for extinct comets and if the existence of active comets in Encke-like orbits is regarded as a probable rather than an improbable occurrence then Wetherill surmises that the cometary source of Apollo-like objects could be as high as 100 per million years. Injection from the asteroid belt, caused by planetary perturbations, leads to an estimated injection rate of about 1.5 per million years. The conclusion drawn is that cometary Apollos exceed asteroidal Apollos by about 10:1 and disagrees completely with the ideas of Kresak and Shoemaker.

In the next section we shall investigate the extent of our knowledge of the asteroid and comet populations. It will be seen then that the supposition that these are adrift by an order of magnitude or two is far from unreasonable. Consideration must also be made of the relative efficiency, as far as crater production is concerned, of asteroids and cometary nuclei. The objects can have very similar kinetic energies, the basic differences being density and strength. Cometary nuclei have low densities of about 1 g cm^{-3} (Hughes 1974) and also very low strength in comparison to asteroids. They have a larger surface area to mass ratio and thus small comets suffer more atmospheric retardation than small asteroids (Tunguska illustrates that a $5 \times 10^{10} \text{ g}$ cometary nuclei could only reach a point 8.5 km up from the Earth's surface before massive energy loss). It is to be expected that cometary nuclei are less efficient at crater production than are asteroids.

ASTEROID AND COMET SIZE DISTRIBUTION

The mass of an astronomical object is an extremely awkward quantity to measure and usually depends on the careful analysis of the perturbing effect that the gravitational field of the unknown mass body has on the orbital motion of a body of known mass. Clearly this is a nigh on impossible task for both asteroids and comets. For asteroids this problem is overcome by estimating their diameter and then making assumptions as to shape (all spherical) and densities (all about 3 g cm^{-3}). Diameters are obtained by using equation (10). This equation simply relates the brightness of an asteroid to its visible surface area and the albedo. The albedo can be inferred either by using the relation between linear polarization and albedo (Ververka 1971) or by investigating the thermal balance. A fraction A (the geometric albedo) of the sunlight hitting the surface of an asteroid is reflected. The complementary fraction $(1 - A)$ is absorbed, heats the surface and is reradiated in the infrared. Measurements of the visual brightness and the infrared flux yield the albedo. The dependence of the two measured quantities on phase angle, surface roughness and asteroid spin rate produces a 20% uncertainty in the albedo and a subsequent 10% uncertainty in diameter. (As asteroids are non-spherical the term diameter actually refers to the effective diameter such that the mean cross-sectional area is $\pi D^2/4$.) Asteroids seem to fall into four albedo classes, carbonaceous $\bar{p}_v = 0.035$, silicaceous $\bar{p}_v = 0.15$, metal-rich $0.08 < \bar{p}_v < 0.15$ and enstatite metal-free, which have high albedos. The numbers of observed and measured asteroids are plotted as a function of diameter in figure 6. Unfortunately the data set is far from complete. Observational selection favours three types of asteroids, those with large diameters, those with high albedos and those with small semi-major axes (these get closer to the Earth). A dividing line between complete and none complete of $D = 250 \text{ km}$ seems to be reasonable. Only 14 asteroids have $D > 250 \text{ km}$. For asteroids smaller than this it becomes much easier to detect the S asteroids than the darker C types.

The cumulative number, N , of observed asteroids having diameters greater than D is plotted as a function of D in figure 7. These data, which come from *Bowell et al.* (1978) seem to have three distinct trends. We can represent $D > 260 \text{ km}$ by

$$\lg N = 5.16 - 1.73 \lg D. \quad (11)$$

The gradient (-1.73 in this case) is equal to $3(1 - s)$ where s , the mass distribution index, equals 1.58 ($m > 2.8 \times 10^{22} \text{ g}$). We can represent $150 < D < 260 \text{ km}$ by

$$\lg N = 9.99 - 3.72 \lg D, \quad (12)$$

which is equivalent to a mass distribution index of 2.24 ($5 \times 10^{21} \text{ g} < m < 2.8 \times 10^{22} \text{ g}$).

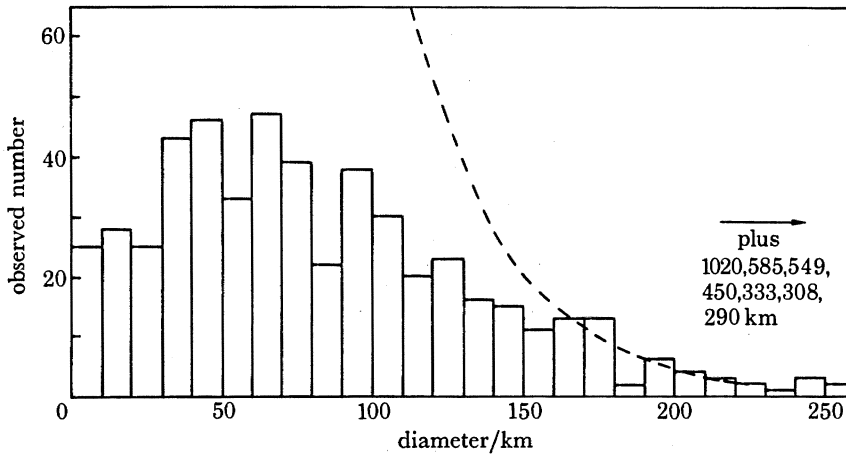


FIGURE 6. A histogram showing how the number of asteroids (523 in total), with accurately determined diameters, vary as a function of diameter. The *general form of the actual distributions* (dashed line) comes from the fit to the cumulative number – diameter line labelled ‘Hughes’ in figure 7. Asteroid data comes from *Bowell et al.* (1978).

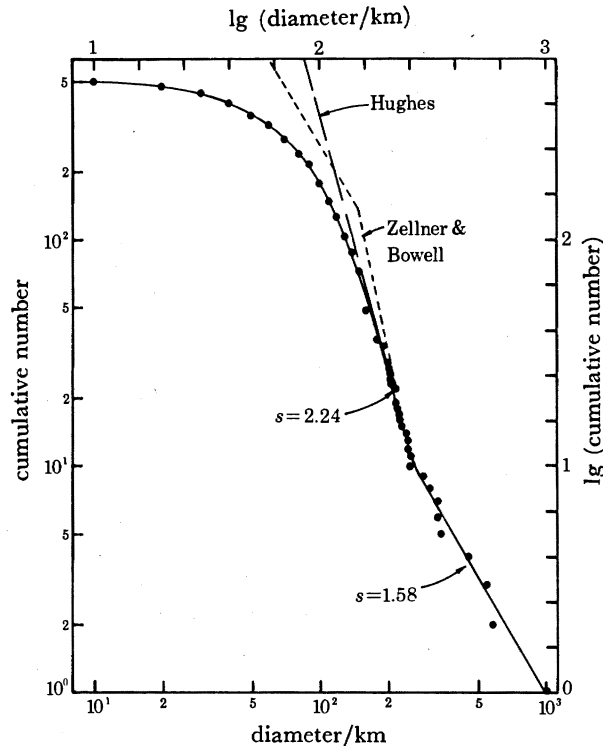


FIGURE 7. The cumulative number of asteroids with diameters greater than D , as a function of D ; s refers to the mass distribution indices of the linear portions of the curve. The dashed line labelled Zellner & Bowell has been generated from data given in their 1977 paper.

For diameters below 150 km the problems of observational selection become nigh on unsurmountable. Obviously there are many more asteroids present in the asteroid belt and in Earth-crossing orbits than have been detected. How many more is still open to debate. A wanton extrapolation of the linear relation given in equation (12) to smaller diameters would be incorrect. Mass distribution indices greater than 2.0 indicate that the majority of the mass of the

total distribution is made up of small objects. This is very unlikely for the asteroids simply because their lifetime in the Solar System is a function of size. Smaller asteroids fragment more frequently than the large ones and thus exist for a shorter time. The flux of impacting objects per unit area to all the asteroids will be approximately constant. Turner (1979) assumed that the fragmentation probability per unit time is proportional to the cross-sectional area of the body being fragmented and to the number density of smaller bodies within the inner Solar System capable of fragmenting it. His conclusions were that the lifetime was proportional to $(\text{mass})^{\frac{1}{2}}$ (i.e. $(\text{diameter})^{\frac{1}{2}}$) and, from meteorite-dating data, that a 100 kg body had a free space lifetime of about 10^7 a. This is equivalent to the relation

$$\tau = 5 \times 10^8 D^{\frac{1}{2}},$$

where τ is the asteroids lifetime in years and D is its diameter in kilometres. This collision lifetime exceeds the age of the Solar System for asteroids with $D > 100$ km.

Quite a few attempts have been made to overcome the problem of observational selection, two recent ones being by Morrison (1977*b*) and Zellner & Bowell (1977). Both attempts apply corrections to the observed numbers, the asteroid belt being divided in three zones for this purpose (2.0–2.5, 2.5–3.0 and 3.0–3.5 AU). Morrison stresses the fact that the ratio of C to S asteroids is approximately 7:1 and that this ratio is independent of solar distance and asteroid absolute magnitude. He also finds that the mass distribution changes at a diameter of about 150 km, this being equivalent to the bump that was prominent in the McDonald survey magnitude–number distribution (see van Houten 1971) at about 9.0 magnitude. The Zellner & Bowell corrected data line is shown in figure 7 together with a more simplified extrapolation labelled ‘Hughes’. The conclusion of Zellner & Bowell does not suffer from a mass excess of small asteroids inherent in the extrapolation to smaller sizes of a distribution with mass index 2.24. The Hughes curve was used to obtain the ‘general form of the actual distribution’ shown in figure 6.

Similar problems of data incompleteness occur when one considers comets. The distribution of comets as a function of their absolute magnitude, H_{10} , is shown in figure 8 (see Hughes & Daniels 1980). The Newburn mass–magnitude relation (8) has been used to obtain the upper abscissa. The comets have been divided into two groups according to orbital period: 104 have periods less than 200 a and are members of the planetary family (the mean period of this group is about 7.9 a); 522 have periods in excess of 200 a. The vast majority of this latter group have only been observed once. Crudely it can be assumed that the $p < 200$ a comets have already undertaken many perihelion passages (more than the $p > 200$ a group) and are thus well on the way to decay. In evolutionary terms the $p > 200$ a group can be regarded as ‘young’ whereas the $p < 200$ a group would be ‘middle aged’. The $p > 200$ a curve is linear over the range $6 > H_{10} > -2$ ($\text{mass} > 4 \times 10^{16}$ g, diameter > 4 km) and this can tentatively be taken to indicate that very few comets in this range are overlooked by observers on Earth. In this range it is found that

$$N \propto 2.02^{H_{10}},$$

a relation that is equivalent to a mass distribution index of 1.76. Unfortunately there is considerable uncertainty in this distribution index, this being due to the tentative nature of the mass–magnitude relation given in equation (8). A standard deviation of ± 0.2 is reasonable.

The deviation from linearity of the $p > 200$ a curve for $H_{10} > 6$ is due mainly to the fact that faint comets are easily overlooked. Many small comets are obviously present and it is just unfortunate that our knowledge of the comet population with diameter below 4 km is incomplete.

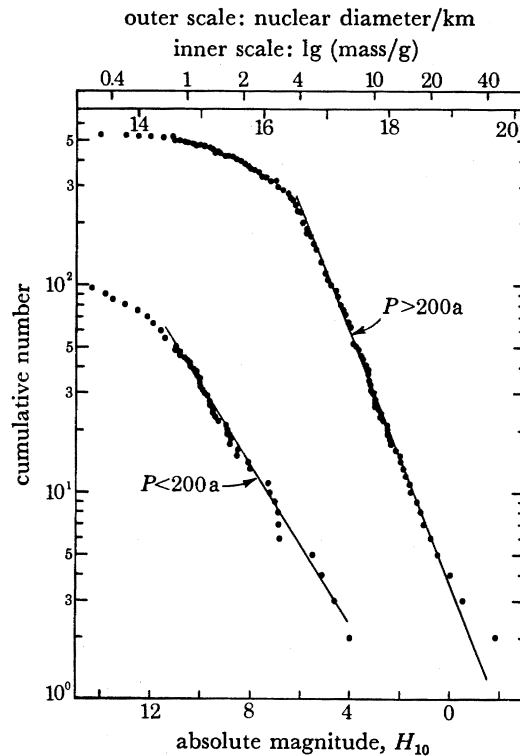


FIGURE 8. The cumulative number of comets having absolute magnitudes brighter, and nuclear masses and diameters greater, than the values given on the abscissa; P refers to the orbital periods of the comet.

The largest comet in the observed sample of 522 has an H_{10} of -3 and thus a mass of about 1.6×10^{20} g. This is definitely not the upper limit of cometary masses. If for example there are somewhere in the region of 10^{11} comets in the Solar System and these obey the relation illustrated by the $p > 200$ a curve in figure 8 then the largest comet would have a mass of about 4×10^{30} g. The fact that this is twice the mass of Jupiter should be taken to indicate that wanton extrapolation is not to be encouraged and also that the second assumption is incorrect. A better assumption, but still highly speculative would be that the linear relation in the $D > 4$ km region of the $p > 200$ a curve extends down to some specified minimum comet size. If we let this minimum be say 10 m then the largest of the 10^{11} comets would have a mass of about 2×10^{23} g and a nucleus diameter of about 700 km.

The short-period comet curve in figure 8 differs considerably from the long-period one and indicates that there are basic changes in cometary parameters between 'young' and 'middle aged' comets as well as differences in the probabilities of detection. The $p < 200$ a group deviates from linearity at a higher magnitude (*ca.* 11) than does the $p > 200$ a group. The main reason for this must be because they are easier to discover, their low periods giving an Earth-bound observer more chances. The mass distribution of this group is about 1.50, this being lower than the value for the $p > 200$ a group. This decrease is due to the perihelion mass loss being dependent on the size of the nucleus, a factor that varies as the comets evolve.

It is extremely difficult to assess the relative probabilities of the Earth colliding with an asteroid, a $p > 200$ a comet and a $p < 200$ a comet. The facts that 2118 asteroids have been observed well enough to give accurate orbital parameters as opposed to 522 long period comets

and 104 short period comets is little help. These numbers depend drastically on such questions as 'Is it easier to observe an asteroid than a comet?', and 'Are more astronomers interested in asteroids as opposed to comets?'. In the main, asteroids are faint objects. Comets vary enormously in brightness, being much dimmer than asteroids at aphelion but being briefly much brighter as they pass perihelion. Figures 6 and 8 represent only those comets and asteroids that have been seen from Earth. What is needed is the distribution of the objects that hit the Earth. Notice that the observed comets are much less massive than the observed asteroids. The biggest observed cometary nucleus has a diameter of about 60 km. Of the asteroids represented in figure 6, 62% are larger than this. I would feel happier with the thesis that Apollo and Amor objects are the remains of decayed cometary nuclei if observed comets were in general larger than observed asteroids. Other reasons for not liking this thesis are given in Hughes (1980*a*).

CONCLUSIONS

Even though our knowledge of asteroidal and cometary statistics is far from complete it is interesting to note that relative quantities (i.e. ones that do not depend on absolute numbers) such as the mass distribution indices, agree fairly well with the indices predicted for the objects responsible for the production of craters on the Earth. The values are: asteroids ($m > 2.8 \times 10^{22}$ g) 1.58, asteroids (5×10^{21} g $< m < 2.8 \times 10^{22}$ g) 2.24, long period comets ($m > 4 \times 10^{16}$ g) 1.76, short period comet ($m > 6 \times 10^{14}$ g) 1.50, which are to be compared with the parent bodies of Earth craters that had mass distribution indices in the range 1.50 to 1.60.

It was also concluded that parent body diameter was in the range $\frac{1}{30}$ to $\frac{1}{69}$ of that of the relevant crater. As the largest Earth craters (Sudbury, Ontario, and Vredefort, South Africa) have diameters of about 140 km, the responsible bodies for the crater distributions given in figure 3 lie in the $3 > D > 0.2$ km range. Reference to figures 8 and 6 respectively shows that relatively few comets and even fewer asteroids with nuclei in this size range have been seen. The similarity of the mass distribution indices gives some justification for the extrapolation of the linear portions of the curves in figures 6 and 8 to lower diameters.

It seems reasonable to assume that cometary nuclei, the dirty ice snowballs that give off dust and gas, cannot exist as active objects for any reasonable period of time if their diameters decrease below a value of around 10 m. The same cannot be said of asteroids. Small asteroids obviously do exist and some clues to the population of these objects can be gleaned from the study of meteorite statistics. A meteorite fall is the name given to that fragment of the incident body that survives the passage through the atmosphere and after landing is large enough to be found and picked up. This retrieval is an extremely haphazard process as can be seen in figure 9. No more need be said than that the fall distribution has a striking similarity to the distribution of regions of high population, intensive agriculture and scientific sophistication. Hughes (1980*b*) found that about 3300 meteorites fall to Earth each year. Unfortunately only six on average are retrieved. The flux of meteorites to the whole surface of the Earth each year is given by

$$\lg \phi_S = 6.61 - 0.90 \lg M_e \quad (13)$$

and

$$\lg \phi_I = 5.57 - 0.82 \lg M_e, \quad (14)$$

where M_e is the retrieved mass in grams and subscripts S and I refer to stones and irons respectively. Equations (13) and (14) are valid over a mass range of 1.6×10^4 g $< M_e < 10^6$ g and lead to mass distribution indices of 1.90 and 1.82 for stone and iron falls respectively. Meteorites have

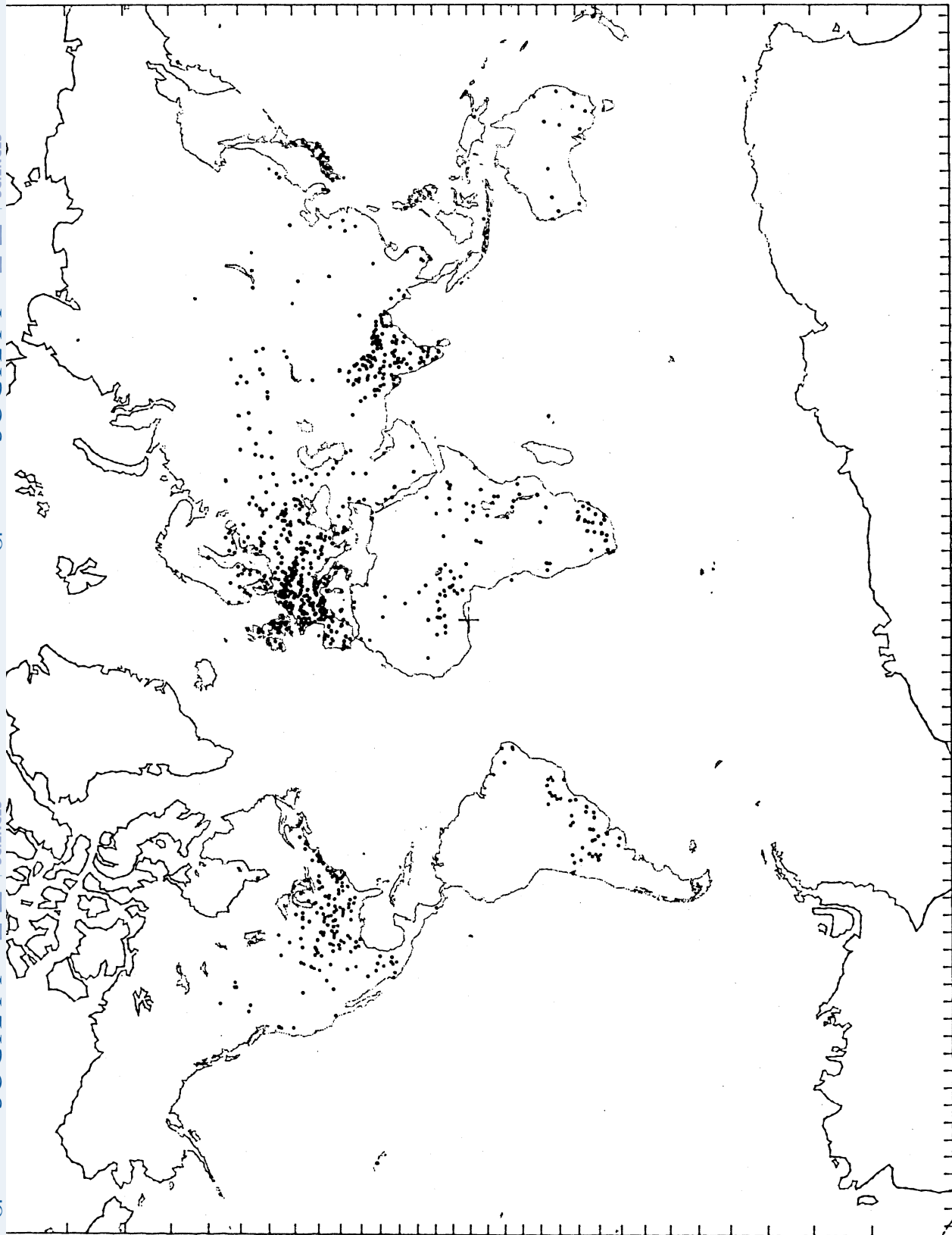


FIGURE 0. A cylindrical Mercator projection of the world map. The dots represent the sites where meteorite falls have occurred. The data originate

suffered massive ablation and retardation (see, for example, Hughes 1980*c*). Their geocentric velocities, in the range 11 to 72 km s⁻¹, have been reduced to a free fall velocity of about 0.07 km s⁻¹. Their mass loss has been considerable. A typical example from the work of ReVelle (1976) is as follows. An incident object with an initial mass of 10⁶ g moving at geocentric velocities of say 11.2, 20, 35 and 68.9 km s⁻¹ will reach the ground with a final mass of 3 × 10⁵, 9 × 10³, 0.3 and 0 g respectively. The atmosphere acts as a strong filter to incident objects, a filter that is highly velocity-dependent as well as being a function of composition, density, mass and entry angle. The mass distribution indices of the retrieved meteorites tell us very little about their parent bodies.

The luminosity of the fireball produced by the ablating object can be related to the initial mass. Ceplecha (1976) found that N , the number of bodies hitting the Earth's atmosphere per year with masses greater than 2 × 10⁸ g, was about 400. McCrosky (1968) used Prairie network fireball data and found that

$$\lg \phi_F = 7.01 - 0.61 \lg m,$$

where m is the interplanetary mass of the object and ϕ_F is the flux to the Earth per year. These data are valid over the range 10³ < m < 10⁶ g.

All the influx relations and data points are given in figure 5. Two main conclusions are obvious. First ablation and retardation in the atmosphere play an important role. This is definitely true in the low mass range and is still probably true at the high, crater producing, end of the figure. Secondly the curve produced by Everhart, assuming collisions with perturbed members of an Oort/Öpik cloud of 10⁹ comets, and the asteroid point due to Shoemaker both lie well below the crater curves, indicating that there are more (10³–10⁴ times more) comets and asteroids than have been assumed.

There is a third general conclusion. The asteroids responsible for meteorite falls and the asteroids and comets that are the parent bodies of craters are all smaller than the mean comet and asteroid observed from Earth. Efforts must be made in the future to discover more about small comets and asteroids. This knowledge, added to information about specific comets and asteroids gleaned from dedicated space missions, should produce a quantum jump in our understanding of the minor bodies in the Solar System.

REFERENCES (Hughes)

- Allen, C. W. 1973 *Astrophysical quantities*. London: Athlone Press.
 Baldwin, R. 1971 *Icarus*, N.Y. **14**, 36–52.
 Bowell, E., Chapman, C. R., Gradie, J. C., Morrison, D. & Zellner, B. 1978 *Icarus*, N.Y. **35**, 313–335).
 Brown, J. C. & Hughes, D. W. 1977 *Nature*, Lond. **268**, 512–514.
 Ceplecha, Z. 1976 In *Interplanetary dust and zodiacal light* (ed. H. Elsässer & H. Fechtig), pp. 385–388. Berlin: Springer-Verlag.
 Dence, M. R., Grieve, R. A. F. & Robertson, P. B. 1977 In *Impact and explosion cratering* (ed. D. J. Roddy, R. O. Pepin & P. B. Merrill), pp. 247–276. Oxford: Pergamon Press.
 Everhart, E. 1969 *Astr. J.* **74**, 735–750.
 Grieve, R. A. F. & Dence, M. R. 1979 *Icarus*, N.Y. **38**, 230–242.
 Grieve, R. A. F. & Robertson, P. B. 1979 *Icarus*, N.Y. **38**, 212–229.
 Hartmann, W. K. 1977 *Scient. Am.* **236**, 84–99.
 Hartmann, W. K. & Wood, C. A. 1971 *Moon* **3**, 3–78.
 Hartung, J. 1976 *Meteoritics* **11**, 187.
 Hey, M. M. 1966 *Catalogue of meteorites*. London: British Museum.
 van Houten, C. J. 1971 In *Physical studies of minor planets* (ed. T. Gehrels), pp. 293–295. N.A.S.A. SP267. Washington, D.C.: N.A.S.A.

- Hughes, D. W. 1974 *J. Br. astr. Ass.* **84**, 272–274.
- Hughes, D. W. 1980a *Nature, Lond.* **286**, 10–11.
- Hughes, D. W. 1980b In *Solid particles in the Solar System* (ed I. Halliday & B. A. McIntosh), pp. 207–210. Dordrecht: D. Reidel.
- Hughes, D. W. 1980c *Nature, Lond.* **288**, 118.
- Hughes, D. W. & Daniels, P. A. 1980 *Mon. Not. R. astr. Soc.* **191**, 511–520.
- Hutchison, R., Bevan, A. W. R. & Hall, J. M. 1977 *Appendix to the catalogue of meteorites*. London: British Museum.
- Kresak, L. 1978a *Bull. astr. Insts Csl.* **29**, 103–114.
- Kresak, L. 1978b *Bull. astr. Insts Csl.* **29**, 114–125.
- McCrosky, R. E. 1968 *Spec. Rep. Smithson. astrophys. Obs.* no. 280.
- Morrison, D. 1977a In *Comets, asteroids and meteorites* (ed. A. H. Delsemme), pp. 177–184. University of Toledo.
- Morrison, D. 1977b *Icarus, N.Y.* **31**, 211.
- Neukum, G. & Wise, D. U. 1976 *Science, N.Y.* **194**, 1381–1387.
- Öpik, E. J. 1951 *Proc. R. Irish Acad. A* **54**, 165–199.
- ReVelle, D. O. 1976 *Nat. Res. Council, Can., planet. Sci.* SR-76-1, July 1976.
- Shoemaker, E. M., Williams, J. G., Helin, E. F. & Wolfe, R. F. 1979 In *Asteroids* (ed. T. Gehrels), pp. 253–282. University of Arizona Press.
- Turner, G. 1979 *Proc. lunar Planet. Sci. Conf. 10th (Geochim. cosmochim. Acta, Suppl. 11)*, pp. 1917–1941.
- Vdovykin, G. P. 1973 *Space Sci. Rev.* **14**, 758.
- Ververka, J. 1971 *Icarus, N.Y.* **15**, 11.
- Wetherill, G. W. 1976 *Geochim. cosmochim. Acta* **40**, 1297–1317.
- Wetherill, G. W. 1979 *Icarus, N.Y.* **37**, 96–112.
- Wood, J. A. 1979 *The Solar System*. Englewood Cliffs, N.J.: Prentice-Hall.
- Zellner, B. & Bowell, E. 1977 In *Comets, asteroids and meteorites* (ed. A. H. Delsemme), pp. 185–197. University of Toledo.